

# Continuous control of an underground loader using deep reinforcement learning

Sofi Backman<sup>1</sup>, Daniel Lindmark<sup>1</sup>, Kenneth Bodin<sup>1,2</sup>, Martin Servin  
(martin.servin@umu.se)<sup>1,2</sup>, Joakim Mörk<sup>1</sup>, and Håkan Löfgren<sup>3</sup>

<sup>1</sup>Algoryx Simulation AB, <sup>2</sup>Umeå University, <sup>3</sup>Epiroc AB

## Abstract

Reinforcement learning control of an underground loader is investigated in simulated environment, using a multi-agent deep neural network approach. At the start of each loading cycle, one agent selects the dig position from a depth camera image of the pile of fragmented rock. A second agent is responsible for continuous control of the vehicle, with the goal of filling the bucket at the selected loading point, while avoiding collisions, getting stuck, or losing ground traction. It relies on motion and force sensors, as well as on camera and lidar. Using a soft actor-critic algorithm the agents learn policies for efficient bucket filling over many subsequent loading cycles, with clear ability to adapt to the changing environment. The best results, on average 75% of the max capacity, are obtained when including a penalty for energy usage in the reward.

## 1 Introduction

Load-Haul-Dump (LHD) machines are used for loading blasted rock (muck) in underground mines, hauling the material to trucks or shafts, where it is dumped. Despite moving in a well confined space, with only a few degrees of freedom to control, LHDs have proved difficult to automate. Autonomous hauling, along pre-recorded paths, and dumping is commercially available but the loading sequence still rely on manual control. It has not yet been possible to reach the loading performance of experienced human operators. The best results have been achieved with admittance control [1], where the forward throttle is coordinated with the bucket lift and curl, using the measured dig force, to fill the bucket while avoiding wheel slip. The motion and applied forces must be carefully adapted to the state of the muck pile, which may vary significantly because of variations in the material and as consequence of previous loadings. Operators use visual cues for controlling the loading, as well as auditory and tactile when available. The

performance between operators varies a lot, indicating the complexity of the bucket filling task.



Figure 1: Image from a simulation of the LHD scooping muck from the pile. The right image show a top-view with the position of the lidar (five rays) and camera indicated.

In this work, we explore the possibility of autonomous control of an LHD using deep reinforcement learning (DRL), which has been proven useful for visuomotor control tasks like grasping objects of different shape. To test whether a DRL controller can learn the task of efficient loading, adapting to muck piles of variable state, we perform the following test.

A simulated environment is created, featuring a narrow mine drift, dynamic muck piles of different initial shape, and an LHD equipped with vision, motion and force sensors, as available on real machines. A multi-agent system is designed to control the LHD towards a mucking position, loading the bucket, and breaking out from the pile. Reward functions are shaped for productivity, energy efficiency, avoiding wall collisions, and wheel slip. The agent’s policy network is trained using the Soft-Actor-Critic algorithm, with a curriculum setup for the mucking agent. Finally, the controller is evaluated on 953 loading cycles.

## 2 Related work

The key challenges in automation of earthmoving machines were recently described in [2]. An overview of the research from the late 1980’s to 2009 is found in [3]. Previous research has focused on computer vision for characterizing the pile [4, 5, 6], motion planning of bucket filling trajectories [7, 4, 8, 9], and of loading control. The control strategies can be divided in trajectory control [10, 8] or force-feedback control [11, 12]. The former aims to move the bucket along a pre-defined path, which is limited to homogeneous media such as dry sand and gravel. The latter regulates the bucket motion based on feedback of interaction forces, thus making it possible to respond to material inhomogeneities and loss of ground traction. One example of this is the admittance control scheme, proposed in [12], refined and tested with good results at full scale in [13]. However, the method require careful tuning of the control parameters and it is difficult to automatically adjust the parameters to a new situation, an issue addressed in [1] using iterative learning control [14]. Artificial intelligence (AI) based methods includes fuzzy logic for wheel loader action selection [15] and digging control [16] using feed-forward neural networks for modeling digging resistance and machine dynamics. Automatic bucket filling by learning from demonstration was recently demonstrated in [17, 18, 19], and extended in [20] with a reinforcement learning algorithm for automatic adaptation of learned model to a new pile environment. A first use of reinforcement learning

to control a scooping mechanism was recently published [21]. Using the actor-critic, Deep Deterministic Policy Gradient algorithm, an agent was trained to control a three-degrees of freedom mechanism to fill a bucket. The study [21], did not consider the use of high-dimensional observation data for adapting to variable pile shapes, selecting a mucking position and steering towards it, repeated and energy efficient scooping while avoiding wheel slip.

## 3 Simulation Model

The simulated environment consist of an LHD and a narrow underground drift with a muck pile, see Fig. 1 and the supplementary video material. The environment was created in Unity [22] using the physics plugin AGX Dynamics for Unity [23, 24]. The vehicle model consists of a multibody system with a drivetrain and compliant tyres. The model was created from CAD-drawings and data sheets of the ScoopTram ST18 from Epiroc [25]. It consists of 21 rigid bodies and 27 joints whereof 8 are actuated. The mass of each body was set to match the 50 tonnes vehicle’s center of mass. Revolute joints model the waist-articulation, wheel axles, bucket and boom joints, and prismatic joints are used for the hydraulic cylinders, with ranges set from the data sheets.

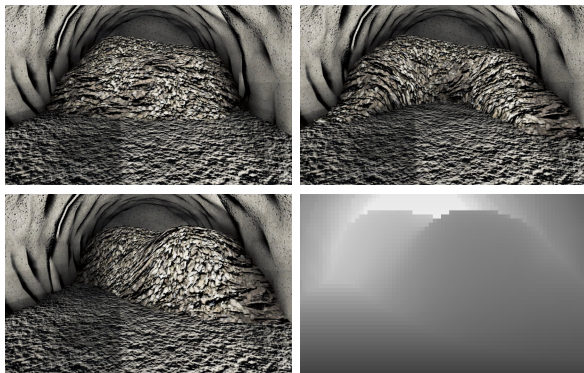


Figure 2: Sample camera images of the initial piles, referred to as convex (upper left), concave (upper right) and right-skewed (lower left), also shown in depth camera view in the lower right image.

The drivetrain consists of a torque curve engine, followed by a torque converter and a gearbox. The power is then distributed to the four wheels through a central-, front- and rear-differential. The torque curve and gear ratios are set to match the real vehicle data. The hoisting of the bucket is controlled by a pair of boom cylinders and the tilting by a tilt cylinder and Z-bar linkage. The hydraulic cylinders are modeled as linear motor constraints with maximum force limited by the current engine RPM. That is, a closed loop hydraulic system was not modelled.

The drift is 9m wide and 4.5m tall with a rounded roof. The muck pile is modeled using a multiscale real-time model [24], combining continuum soil mechanics, discrete elements, and rigid multibody dynamics for realistic dig force and soil displacement. Sample piles are shown in Fig. 2, as observed by the cameras on the vehicle. The LHD is also equipped with 1D lidar, measuring the distance to the tunnel walls and the pile in five directions, indicated in Fig. 1. The muck is modeled with mass density  $2700 \text{ kg/m}^3$ , internal friction angle  $50^\circ$  and cohesion 6 kPa. Natural variations are represented by adding a uniform perturbation of  $\pm 2000 \text{ kg/m}^3$  to the mass density having the penetration force scaling range randomly between 5-8 for each pile. Variations of sample pile shapes is ensured by saving pile shape generations. After loading 10 times from an initial pile, the new shape is saved into a pool of initial pile shapes and tagged as belonging to generation 1. A state inheriting from generation 1 is tagged as generation 2, and so on.

The simulations run with a 0.02 s timestep and default settings for the direct-iterative split solver in AGX Dynamics [23]. The grid size of the terrain is set to 0.32 m.

## 4 ML-Controller

The task of performing several consecutive mucking trajectories requires long term planning of how the state of the muck pile develops. Training a single agent to handle both high-level planning and continuous motion control was deemed too hard. Therefore, two cooperating agents were trained, a *Mucking Position Agent* (MPA) and a *Mucking Agent* (MA). The

former chooses the best mucking position, once for each loading cycle, and the latter controls the vehicle at 16 Hz to efficiently muck at the selected position. To train the agents, we used the implementation of Soft Actor-Critic (SAC) [26] in ML-Agents [27]. SAC is an off-policy DRL algorithm that trains the policy to maximize a trade-off between expected return and policy entropy, as seen in the augmented objective,

$$J(\pi) = \mathbb{E}_\pi \left[ \sum_t r(\mathbf{s}_t, \mathbf{a}_t) - \alpha \log(\pi(\mathbf{a}_t | \mathbf{s}_t)) \right]. \quad (1)$$

Including the policy entropy in the objective function contributes to exploration while training and results in more robust policies that generalize to unseen states better. Combined with off-policy learning, it makes SAC a sample efficient DRL algorithm, which will be important for the MPA, as explained below.

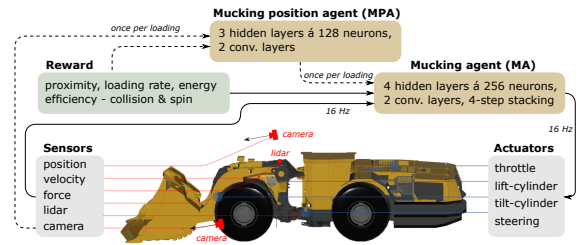


Figure 3: Illustration of the ML-controller and how the agents cooperate.

Fig. 3 illustrates the relation between the two agents. The MPA’s observation is a depth camera, at a fixed position in the tunnel, with resolution  $84 \times 44$ . The action is to decide at what lateral position in the tunnel to dig into the pile. This decision is made once per loading.

The MA’s task is to complete a mucking cycle. This involves the following: *approach the pile* to reach the mucking position with the vehicle straight for maximum force and avoiding collision with the walls; *fill the bucket* by driving forward and gradually raising and tilting the bucket, while avoiding wheel slip; and finally *decide to finish and breakout* by tilting the bucket to max and holding it still.

The MA observes the pile using depth cameras simulated using rendered depth buffer, and lidar data

simulated using line-geometry intersection. As well as a set of scalar observations consisting of the positions, velocities, and forces of the actuated joints, the RPM of the center shaft, and the lateral distance between bucket tip and the target mucking position. The scalar observations are stacked four times, meaning that we repeat observations from previous timesteps, giving the agent a short-term "memory" without using a recurrent neural network. The actions include the engine throttle, and the target velocities of each hydraulic cylinder controlling the lift, tilt, and the articulated steering of the vehicle. Note, that the target velocity will not necessarily be the actual velocity achieved by the actuator, due to limited available power and resistance from the muck.

The MA's neural network consists of four hidden fully connected layers of 256 neurons each. The depth camera data is first processed by two convolutional layers followed by four fully connected layers, where the final layer is concatenated together with the final layer for the scalar observations. The MPA's neural network differs only for the fully connected layers, where we instead use three layers with 128 neurons each. Both the MA and the MPA were trained with a batch size of 256, a constant learning rate of  $1e-5$ , a discount factor  $\gamma = 0.995$ , updating the model once per step, and initial value of the entropy coefficient  $\alpha$  in Eq. (1) set to  $\alpha = 0.2$ . The buffer size is reduced from  $3e5$  for the MA, to  $1e5$  for the MPA.

The MA reward function depends on the fulfillment of the chosen mucking position  $r_t^p = 1 - \min\left(\frac{1}{4m}|x_{\text{target}} - x_{\text{bucket}}|, 1\right)^{0.4}$ , the increment in bucket fill fraction  $r_t^l = l_t - l_{t-1}$  and the work done by the engine and hydraulic cylinders since the last action  $p_t^w = (p_{\text{tilt}} + p_{\text{lift}} + p_{\text{steer}} + p_{\text{engine}}/5)$ . If the vehicle come in contact with the wall or if any wheel is spinning, this is registered by setting the indicators  $C = 0$  and  $W = 0$ , respectively. Otherwise these have value 1. The complete reward function is

$$r_t^{\text{MA}} = w_1 C W r_t^p r_t^l - w_2 p_t^w, \quad (2)$$

with weight factors  $w_1 = 100$  and  $w_2 = 10^{-6} \text{ J}^{-1}$ . This reward favors mucking at the target position and increasing the volume of material in the bucket compared to the previous step, while heavily penal-

ising collision with walls or wheel spin. Finally, subtracting the current energy consumption encourage energy saving strategies and mitigates unnecessary movements that do not increase the possibility of current or future material in the bucket. Additionally, a bonus reward is given if the agent reaches the end-state,  $r_T = 10r_p l_T$ , that is the position reward times the final bucket fill fraction. This is to encourage the agent to finish the episode when it is not possible to fill the bucket any further, except by reversing and re-entering the pile.

The reward for the mucking position agent is the final fill fraction achieved by the mucking agent, times a term that promote keeping a planar pile surface,  $s_t = e^{-d^2/2}$ , where  $d$  is the longitudinal distance between the innermost and outermost points on the edge of the pile, indicated in Fig. 1. The reward become

$$r_t^{\text{MPA}} = l_t s_t. \quad (3)$$

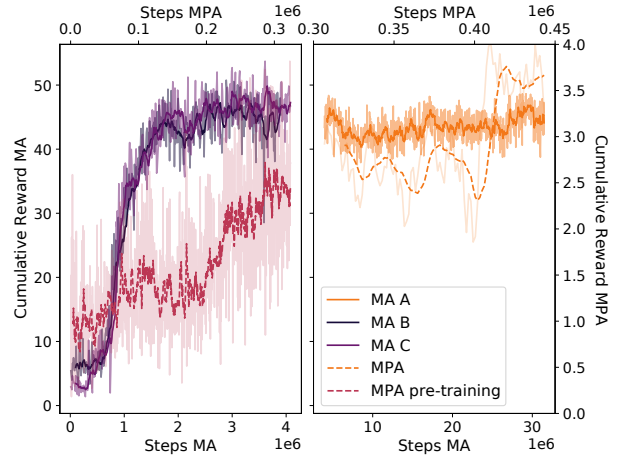


Figure 4: The cumulative reward for the three configurations of ML-controllers tested.

The MPA receives a reward for each loading completed by the MA. Due to the comparatively slow data collection, a sample-efficient DRL-algorithm is important. The two agents were trained in two steps, first separately and then together. The mucking agent was trained with a curriculum setup, us-

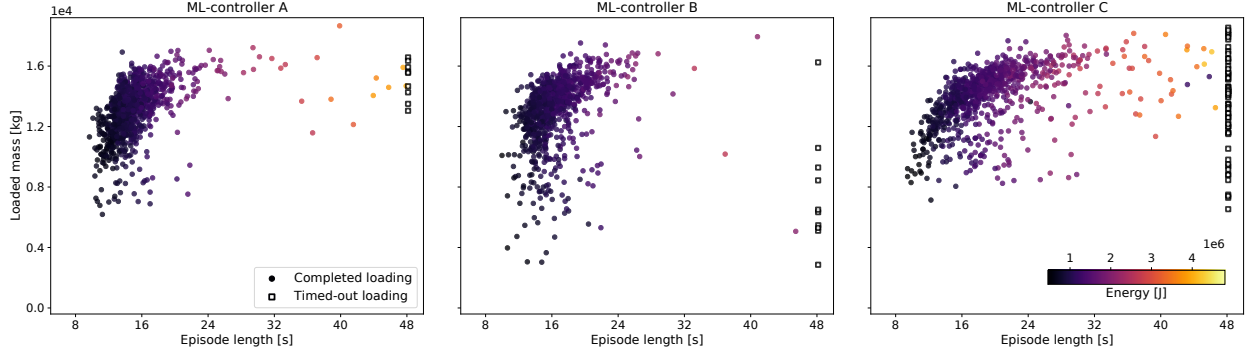


Figure 5: The performance of the three tested ML-controllers from 953 loading cycles.

ing three different lessons. Each lesson increases the number of consecutive loading trajectories by five, from 10 to 20, and the number of pile shape generations by 1, from 0 to 2. During pre-training each trajectory targeted a random mucking position on the pile. The MPA was first trained with the pre-trained MA, without updating the MA model. When the MPA showed some performance we started updating the MA model together with the MPA model. The model update rate for both models is then limited by the MPA model.

## 5 Results

We compare the performance of three different configurations of the ML-controller, denoted A, B, and C. Controller A combines the MPA and MA with the rewards functions (2) and (3). For comparison, controller C does not include the penalty for energy usage in Eq. (2) and neither of controller B or C use the MPA. The training progress is summarized in Fig. 4. Controller B and C was trained for the same amount of steps and using the same hyperparameters, while A continued to train from the state at which B ended. For each ML-controller we collected data from 953 individual loadings. Each sample is one out of twenty consecutive loadings starting from one of the four initial piles. The pile was reset after twenty loadings. During testing, the muck pile parameters are set to the default values, except for the

mass density which is set as the upper limit, so that one full bucket is about 17.5 tonnes. The loaded mass is determined from the material inside the convex hull of the bucket. This ensures we do not overestimate mass in the bucket, by including material that might fall off when backing away from the pile.

The mucking agents learn the following behaviour, which is also illustrated by the supplementary video material. The Mucking Agent starts with lining up the vehicle towards the target mucking position with the bucket slightly raised from the ground and tilted upwards. When the vehicle approaches the mucking pile, the bucket is brought flat to the ground and driven into the pile at a speed of approximately 1.6 m/s. Soon after entering the pile, the MA starts lifting and tilting the bucket. This increases the normal force, which provides traction to continue deeper into the pile without the wheels slipping. After some time the vehicle start breaking out from the pile with the bucket fully tilted.

The loaded mass in the bucket at the end of each episode is plotted in Fig. 5 with the corresponding episode duration and energy use. The majority of the trajectories are clustered in the upper left corner of high productivity (ton/s). Each of the three controllers have some outliers, loadings with low mass and/or long loading time. If the mucking agent does not reach the final state of breaking out with the bucket fully tilted within 48 s, the loading is classified as failed. The common reason for timing out is the vehicle being stuck in the pile with a load too



large for breaking out. The ML-controller C, not rewarded for being energy efficient, has longer loading duration and is more prone for getting stuck.

The mean productivity and energy usage for ML-controller A, B, and C are presented in Table 1. The failure ratio and mucking position error are also included. Comparing controller B and C, we observe that the energy penalty in the reward functions leads to 21% less energy consumption, 7% increase in productivity, and reduces the failure ratio from 7% to 1%. We conclude that controller A and B learn a mucking strategy that actively avoids entering states that lead to high energy consumption and delayed breakout. On average the loaded mass is between 75 – 80% of the vehicle’s capacity of 17.5 ton. The energy use is 1.4 – 1.9 times larger than the energy required for raising that mass 4 m up. That is reasonable considering the soil’s internal friction and cohesion, and that the internal losses in the LHD is not accounted for.

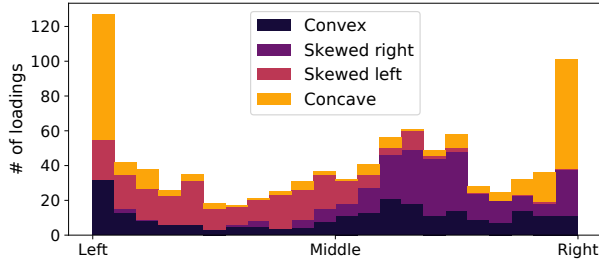


Figure 6: The distribution of target positions chosen by MPA for each of the four starting piles.

ML-controller A has 9% higher productivity than controller B, that muck at random positions, and use 4% less energy. This suggests that the mucking position agent has learned to recognize favorable mucking positions from the depth image. Confirming this, Fig. 6 shows the distribution of the mucking position for the four different starting piles. For the starting pile skewed to the left, MPA chooses to muck more times at the left part of the tunnel, an action that involves smaller digging resistance to fill the bucket and has the effect of making the pile more evenly shaped. The same pattern is true for the pile skewed to the right. For the concave pile the majority of the targets

are at the left or right edge, effectively working away the concave shape. For the convex shape, the mucking position is more evenly distributed. Fig. 7 shows the evolution of the loaded mass, using ML-controller A, over the sequence of 20 repeated muckings from the initial piles. There is no trend of degrading mucking performance. This shows that the MPA acts to preserve or improve the state of the pile, and that the ML-controller has generalised to the space of different mucking piles.

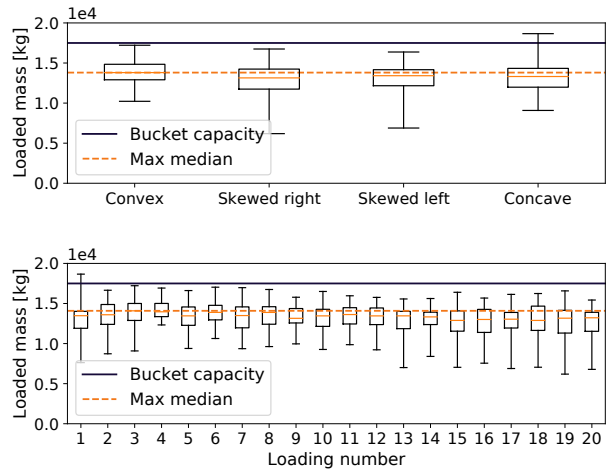


Figure 7: Boxplot of the loaded mass during repeated mucking using ML-controller A. The whiskers shows the max and min value.

The target mucking position chosen by the MPA is not guaranteed to be the position that the LHD actually mucks at, since we expect an error in MA precision, and it can weigh the importance of mucking at the target position against the importance of filling the bucket with low energy cost. The mean difference between the target and actual mucking position for ML-controller A is  $0.014 \pm (0.15)$  m, which is 0.4% of the bucket width.

## 6 Conclusions

We have found that it is possible to train an ML-controller to use high-dimensional sensor data, from

Table 1: Mean performance for the different ML-controllers.

ML-Controller		Mass [ton]	Productivity [ton/s]	Energy usage [MJ]	Position error [m]	Failure
A	all loadings	13.2( $\pm 1.8$ )	0.87( $\pm 0.15$ )	1.10( $\pm 0.5$ )	0.01( $\pm 0.15$ )	1%
	completed loadings	13.2( $\pm 1.8$ )	0.88( $\pm 0.14$ )	1.08( $\pm 0.39$ )	0.01( $\pm 0.15$ )	
B	all loadings	13.1( $\pm 2.3$ )	0.80( $\pm 0.16$ )	1.12( $\pm 0.26$ )	0.11( $\pm 0.20$ )	1%
	completed loadings	13.1( $\pm 2.2$ )	0.81( $\pm 0.14$ )	1.12( $\pm 0.24$ )	0.11( $\pm 0.20$ )	
C	all loadings	14.0( $\pm 2.0$ )	0.73( $\pm 0.20$ )	1.55( $\pm 0.75$ )	0.08( $\pm 0.23$ )	7%
	completed loadings	14.0( $\pm 1.9$ )	0.76( $\pm 0.16$ )	1.42( $\pm 0.53$ )	0.08( $\pm 0.23$ )	

different domains, without any pre-processing as input to neural network policies, to solve the complex control task of repeated mucking with high performance. Even though the bucket is seldom filled to the max, it is consistently filling the bucket with a good amount from a large different set of pile shapes and properties. It is common for human operators use more than one attempt to fill the bucket when the pile shape is not optimal. A tactic that is not considered here.

Including an energy consumption penalty in the reward function can distinctly reduce the agent’s overall energy usage. This agent learns to avoid certain states that inevitable lead to high energy consumption and risk of failing in completing the task. The two objectives of loading more material and using less energy are competing, as seen in Table 1 with controller C higher mass and controller A lower energy usage. This is essentially a multi-objective optimisation problem that will have a Pareto-front of possible solutions, with different prioritisation between the objectives. In this work, we prioritised by choosing the coefficients  $w_1 = 100$  and  $w_2 = 10^{-6}$  in Eq. (2), but future work could analyse this trade-off in more detail.

A low resolution depth camera observation of the pile surface is enough to train the MPA to recognise good 1D positions, for the MA to target. By choosing the target position the overall production increases and the energy consumption decreases, compared to targeting random positions. Continuing to clear the entire pile using this method, essentially cleaning up and reaching a flat floor, could be an interesting task

for future work.

## Supplementary material

Supplementary material including videos can be found at <https://www.algoryx.se/papers/dr1-loader/>.

## References

- [1] H. Fernando, J. Marshall, and J. Larsson. Iterative learning-based admittance control for autonomous excavation. *Journal of Intelligent & Robotic Systems*, 96(3):493–500, Dec 2019.
- [2] S. Dadhich, U. Bodin, and U. Andersson. Key challenges in automation of earth-moving machines. *Automation in Construction*, 68:212–222, 2016.
- [3] A. Hemami and F. Hassani. An overview of autonomous loading of bulk material. *Proceedings of the 26th ISARC, Austin TX, U.S.A.*, pages 405–411, 2009.
- [4] S. Sarata, Y. Weeramhaeng, and T. Tsubouchi. Approach path generation to scooping position for wheel loader. In *Proceedings of the 2005 IEEE International Conference on Robotics and Automation*, pages 1809–1814, 2005.
- [5] M. Magnusson and H. Almqvist. Consistent pile-shape quantification for autonomous wheel loaders. In *2011 IEEE/RSJ International Confer-*

- ence on *Intelligent Robots and Systems*, pages 4078–4083, 2011.
- [6] C. McKinnon and J. Marshall. Automatic identification of large fragments in a pile of broken rock using a time-of-flight camera. *IEEE Transactions on Automation Science and Engineering*, 11(3):935–942, 2014.
  - [7] S. Singh and H. Cannon. Multi-resolution planning for earthmoving. In *Proceedings. 1998 IEEE International Conference on Robotics and Automation (Cat. No. 98CH36146)*, volume 1, pages 121–126. IEEE, 1998.
  - [8] R. Filla and B. Frank. Towards finding the optimal bucket filling strategy through simulation. In *Proceedings of 15:th Scandinavian International Conference on Fluid Power, June 7-9, 2017, Linköping, Sweden*, 06 2017.
  - [9] D. Lindmark and M. Servin. Computational exploration of robotic rock loading. *Robotics and Autonomous Systems*, 106:117–129, 2018.
  - [10] N. Koyachi and S. Sarata. Unmanned loading operation by autonomous wheel loader. In *2009 ICCAS-SICE*, pages 2221–2225, 2009.
  - [11] W. Richardson-Little and C. J. Damaren. Position accommodation and compliance control for robotic excavation. *Journal of Aerospace Engineering*, 21(1), 2008.
  - [12] J. A. Marshall, P. F. Murphy, and L. K. Daneshmend. Toward autonomous excavation of fragmented rock: Full-scale experiments. *IEEE Transactions on Automation Science and Engineering*, 5(3):562–566, 2008.
  - [13] A. Dobson, J. Marshall, and J. Larsson. Admittance control for robotic loading: Design and experiments with a 1-tonne loader and a 14-tonne load-haul-dump machine. *Journal of Field Robotics*, 34(1):123–150, 2017.
  - [14] D. A. Bristow, M. Tharayil, and A. G. Alleyne. A survey of iterative learning control. *IEEE Control Systems Magazine*, 26(3):96–114, 2006.
  - [15] P. Lever. An automated digging control for a wheel loader. *Robotica*, 19(5):497, 2001.
  - [16] L. Wu. *A study on automatic control of wheel loaders in rock/soil loading*. PhD thesis, The University of Arizona, 2003.
  - [17] S. Dadhich, F. Sandin, U. Bodin, U. Andersson, and T. Martinsson. Field test of neural-



- network based automatic bucket-filling algorithm for wheel-loaders. *Automation in Construction*, 97:1 – 12, 2019.
- [18] E. Halbach, J. Kämäräinen, and R. Ghabcheloo. Neural network pile loading controller trained by demonstration. In *2019 International Conference on Robotics and Automation (ICRA)*, pages 980–986, 2019.
- [19] W. Yang, N. Strokina, N. Serbenyuk, R. Ghabcheloo, and J. Kämäräinen. Learning a pile loading controller from demonstrations. In *2020 IEEE International Conference on Robotics and Automation (ICRA)*, pages 4427–4433, 2020.
- [20] S. Dadhich, F. Sandin, U. Bodin, U. Andersson, and T. Martinsson. Adaptation of a wheel loader automatic bucket filling neural network using reinforcement learning. In *2020 International Joint Conference on Neural Networks (IJCNN)*, pages 1–9, 2020.
- [21] O. Azulay and A. Shapiro. Wheel loader scooping controller using deep reinforcement learning. *IEEE Access*, 9:24145–24154, 2021.
- [22] Unity Technologies. Unity. <https://unity.com>. Version 2019.3.7f1 [Accessed 2021-03-01].
- [23] Algorix. AGX Dynamics. <https://www.algorix.se/agx-dynamics/>, 2020. [Accessed 2020-10-19].
- [24] M. Servin, T. Berglund, and S. Nystedt. A multiscale model of terrain dynamics for real-time earthmoving simulation. In *arXiv/2011.00459*, 2020.
- [25] Epiroc. *ScoopTram ST18 - Specification*, 2019.
- [26] T. Haarnoja, A. Zhou, P. Abbeel, and S. Levine. Soft actor-critic: Off-policy maximum entropy deep reinforcement learning with a stochastic actor, 2018.
- [27] A. Juliani, V.-P. Berges, E. Teng, A. Cohen, J. Harper, C. Elion, C. Goy, Y. Gao, H. Henry, M. Mattar, and D. Lange. Unity: A general platform for intelligent agents. <https://arxiv.org/pdf/1809.02627.pdf>, 2018. [Accessed 2020-06-23].